**NAVAL AIR WARFARE CENTER AIRCRAFT DIVISION
PATUXENT RIVER, MARYLAND**

TECHNICAL INFORMATION MEMORANDUM

REPORT NO: NAWCADPAX/TIM-2016/54

IONIC TRANSPORT THROUGH METAL-RICH ORGANIC COATINGS

by

**Brandy Mobley
Kevin M. Cook
Anna K. Safigan
Noah Wichrowski
Zachary Nega
Victor Rodriguez-Santiago**

19 August 2016

Approved for public release.

DEPARTMENT OF THE NAVY
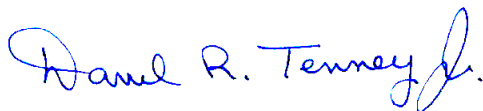NAVAL AIR WARFARE CENTER AIRCRAFT DIVISION
PATUXENT RIVER, MARYLAND

IONIC TRANSPORT THROUGH METAL-RICH ORGANIC COATINGS

by

Brandy Mobley
Kevin M. Cook
Anna K. Safigan
Noah Wichrowski
Zachary Nega
Victor Rodriguez-Santiago

RELEASED BY:

19 Aug 2016

_____
Darrel Tenney / 4.3.4 / DATE
Head, Materials Engineering Division
Naval Air Warfare Center Aircraft Division

NAWCADPAX/TIM-2016/54

REPORT DOCUMENTATION PAGE			Form Approved OMB No. 0704-0188		
Public reporting burden for this collection of information is estimated to average 1 per response, including the time for reviewing instructions, searching existing data sources, gathering and maintaining the data needed, and completing and reviewing this collection of information. Send comments regarding this burden estimate or any other aspect of this collection of information, including suggestions for reducing this burden, to Department of Defense, Washington Headquarters Services, Directorate for Information Operations and Reports (0704-0188), 1215 Jefferson Davis Highway, Suite 1204, Arlington, VA 22202-4302. Respondents should be aware that notwithstanding any other provision of law, no person shall be subject to any penalty for failing to comply with a collection of information if it does not display a currently valid OMB control number. **PLEASE DO NOT RETURN YOUR FORM TO THE ABOVE ADDRESS.**					
1. REPORT DATE 19 August 2016		2. REPORT TYPE Technical Information Memorandum	3. DATES COVERED October 2013-Septermber 2015		
4. TITLE AND SUBTITLE Ionic Transport Through Metal-Rich Organic Coatings			5a. CONTRACT NUMBER		
			5b. GRANT NUMBER		
			5c. PROGRAM ELEMENT NUMBER		
6. AUTHOR(S) Brandy Mobley, Kevin M. Cook, Anna K. Safigan, Noah Wichrowski, Zachary Nega, and Victor Rodriguez-Santiago			5d. PROJECT NUMBER		
			5e. TASK NUMBER		
			5f. WORK UNIT NUMBER		
7. PERFORMING ORGANIZATION NAME(S) AND ADDRESS(ES) Naval Air Warfare Center Aircraft Division Code 4346, Bldg. 2188 48066 Shaw Road, Patuxent River, MD 20670			8. PERFORMING ORGANIZATION REPORT NUMBER NAWCADPAX/TIM-2016/54		
9. SPONSORING/MONITORING AGENCY NAME(S) AND ADDRESS(ES) Naval Air Systems Command (Section 219) 47123 Buse Road Patuxent River, MD 20670-1547			10. SPONSOR/MONITOR'S ACRONYM(S)		
			11. SPONSOR/MONITOR'S REPORT NUMBER(S)		
12. DISTRIBUTION/AVAILABILITY STATEMENT Approved for public release.					
13. SUPPLEMENTARY NOTES					

14. ABSTRACT

Organic coatings are commonly used on aircraft and in the automotive industry to protect against corrosive environments. Although coatings are frequently used today, the mechanisms behind their protective nature are not fully understood. This paper investigates how metal particle volume (MPV) percent, solvent polarity, and resin molecular weight impact corrosion protection of metal-rich organic (MRO) coatings. Following design of experiments (DOE) and Taguchi methodologies, the three parameters investigated, along with their respective levels, were used to generate an orthogonal test matrix of coating formulations. Due to the brittle nature of the coatings, these formulations could not be stand-alone and were sprayed onto filter paper to lend structural support. Using a modified Hitorff cell, the nine independent formulations from the orthogonal matrix were tested for pH and chloride ion concentration levels over time. As the corrosion protection of the coating decreases, chloride ion concentration will increase. Preliminary tests indicate that the effects of MPV percent, solvent polarity, and resin molecular weight can be measured using a modified Hitorff cell set-up, however, no trends can be determined from the data at this time.

15. SUBJECT TERMS

Organic, coatings, metal, particle, Taguchi, matrix, Hitorff cell

16. SECURITY CLASSIFICATION OF:			17. LIMITATION OF ABSTRACT	18. NUMBER OF PAGES	19a. NAME OF RESPONSIBLE PERSON Victor Rodriguez-Santiago
a. REPORT	b. ABSTRACT	c. THIS PAGE			19b. TELEPHONE NUMBER (include area code)
Unclassified	Unclassified	Unclassified	SAR	25	(301) 342-8040

Standard Form 298 (Rev. 8-98)
Prescribed by ANSI Std. Z39-18

SUMMARY

Organic coatings are commonly used on aircraft and in the automotive industry to protect against corrosive environments. Although coatings are frequently used today, the mechanisms behind their protective nature are not fully understood. This paper investigates how metal particle volume (MPV) percent, solvent polarity, and resin molecular weight impact corrosion protection of metal-rich organic (MRO) coatings. Following design of experiments (DOE) and Taguchi methodologies, the three parameters investigated, along with their respective levels, were used to generate an orthogonal test matrix of coating formulations. Due to the brittle nature of the coatings, these formulations could not be stand-alone and were sprayed onto filter paper to lend structural support. Using a modified Hitorff cell, the nine independent formulations from the orthogonal matrix were tested for pH and chloride ion concentration levels over time. As the corrosion protection of the coating decreases, chloride ion concentration will increase. Preliminary tests indicate that the effects of MPV percent, solvent polarity, and resin molecular weight can be measured using a modified Hitorff cell set-up. Based on the results of the DOE, an optimal formulation is identified within the parameter space studied.

Contents

Figures

Tables

ACKNOWLEDGEMENTS

INTRODUCTION

BACKGROUND

Coatings act as thin layers that protect substrates from corrosion and environmental degradation.[1] They take advantage of the mechanical properties of the substrate and introduce desired surface properties.[1] Coatings are prevalent in many forms as corrosion protection systems and include organic paints, inert metallic layers, and protective oxide layers.[2] Although coatings have been commercially used for many years, the design of new coatings and the fundamental aspects of their protective behavior still warrant study, and thus research into the field of coatings is ongoing.[3] These coating systems are typically described as one of three main types: metallic, non-metallic inorganic, and organic.[2] The deciding factor in choosing a coating is the substrate in question, the desired end use for the final product, and the environment in which the final product will be operated. The methods for applying these coatings also vary based on the ability of the substrate to withstand the method and, again, the desired final product. Herein, we discuss the performance of one type of organic coating – metal-rich organic primer – as an ionic and electronic barrier for corrosion protection.

Corrosion prevention and inhibition are major factors in researching and developing coating systems. The electrochemical reactions between materials and their environments lead to the deterioration of the material and its properties.[2] Within organic coatings, three types of protection schemes are available: electrochemical inhibitors, sacrificial coatings, and barrier coatings.[4] Electrochemical inhibitors such as the pigments found in chromates protect the substrate by passivating the metallic surface with an oxide layer. Sacrificial coatings prevent the self-corrosion of the metal substrate through the electrical contact with anodic inhibitors. Barrier coatings prevent water and oxygen from reaching the metal surface, eliminating the components needed for a cathodic reaction to occur. Additionally, organic barrier coatings are protective by preventing current flow between anodic and cathodic regions due to their higher electrical resistance.

While organic coatings are useful in preventing corrosion, some problems exist. Defects within a coating can introduce a direct pathway to the substrate, resulting in localized barrier protection loss. Further barrier protection loss may occur around the localized attack by coating delamination.[5] Cathodic delamination occurs spontaneously in seawater on cathodically polarized surfaces and has been established as a process that promotes degradation of organic coatings.[6] Additionally, barrier layers can experience blistering and delamination due to osmotic pressure.[7]

One subset of organic coatings that offers considerable promise for corrosion protection is metal-rich primers. Metal particle loading of organic systems is of particular interest because current studies have found organic-inorganic hybrid films to be one of the most promising approaches for replacing chromate-based pre-treatments – particularly hexavalent chrome – for high strength structural aluminum parts.[8] These metal-rich primers are organic-based and comprise the three components mentioned above—e.g., binder, pigments, and additives—where one of the additives is metal particles. These particles serve as sacrificial anodes, protecting the substrate metal.[2]

Metal-loaded coatings have an advantageous combination of ductility, deformability, and high dielectric constant attributed to the organic components, as well as stabilized size and strength imparted by the metal particles.[9] When compared to conventional systems that use pigments, metal particles provide more robust corrosion protection and are more economical.[10]

To form these metal-rich primers, an organic coating is loaded with metal particles by adding metal particles to the resin prior to coating application.[9] A typical preparation involves two components, combined in steps – first, resin is mixed with solvent, and second, a curing agent is then mixed with the solvent. Metal particles are measured and added to resin/solvent mixture, then both parts are agitated. The two parts are mixed, then agitated again before application to provide better consistency. Electrochemical impedance spectroscopy (EIS) and scanning kelvin probe microscopy (SKP) have commonly been used to characterize degradation of organic coatings on metals. Barrier protection type coatings apply EIS to characterize interface stability, such as adhesion properties at the interface and water uptake.[1,8, 11]

<u>PURPOSE</u>

In this work, we focus on characterizing metal-rich coating performance via the diffusion of chloride ions, Cl^-, through the films. The migration of these ions indicates the rate of deterioration of the coating and can be easily measured using a chloride-ion selective electrode (ISE). Other studies have used ISEs to evaluate effectiveness of organic coatings; Leidheiser et al. studied how the migration of Cl^-, Na^+, and Cs^+ affected delamination of organic coatings.[8] The diffusion of chloride ions is especially important for metal substrates, as it is well-known that chloride increases corrosion of metals.[3] For metal-loaded primers, it has been established that the coating preparation parameters – molecular weight of the resin, polarity of the solvent, and metal particle volume (MPV) fraction – affect the diffusion properties of the system, but the extent to which each parameter is a factor is unknown. The hypothesis for this work is that chloride ion diffusion acts as an indicator of metal-rich coating performance. The higher the transfer of chloride ions, the less protection afforded by the primer. Therefore, the purpose of this study is to investigate how resin molecular weight, solvent polarity, and volume fraction of metal particles in metal-rich organics (MROs) impact the chloride ion diffusion mechanisms and to identify which variables optimize coating protection. Design of experiment (DOE) methods guided experimental work by isolating critical study parameters and determining an experimental matrix. Testing samples from the generated matrix made possible the determination of the key effects of these parameters and how to best optimize the metal-rich system for corrosion protection.

DISCUSSION

EXPERIMENTAL PROCEDURE

SAMPLE PREPARATION

Samples were intended to be tested independently as free-standing films. Due to the brittle nature of coating systems, samples required additional structural stability to prevent sample deterioration prior to testing. Normally, structural stability is provided by a metallic substrate. To test diffusion mechanisms of the coating independent of the substrate, samples were sprayed onto 2.2 in (5.5 cm) filter paper of medium porosity (a particle retention rate of 5-10 μm) and medium flow rate (60 mL/min.) as shown in Figure 1(a). It was assumed that the filter paper supplied structural support without contributing to or interfering with the coating system properties.

Coating was sprayed onto filter paper as shown in Figure 1(a) to lend structural support, then masked with silicone to prevent solution loss through the filter [Figure 1(b)]. The fully assembled test apparatus is shown in Figure 1(c).
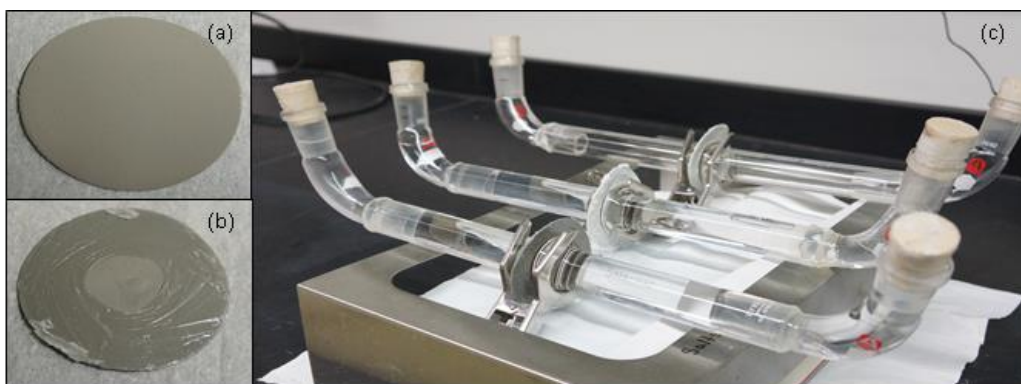

Figure 1: Coating Sprayed onto Filter Paper

DESIGN OF EXPERIMENTS

Within DOE, the Taguchi method reduces product variability to produce a robust design. The Taguchi matrix is a quality control methodology that, when given testing parameters, provides data for a widespread set of combinations without testing every parameter permutation. An L-9 matrix was applied to the three variables being evaluated – molecular weight of the resin, solvent polarity, and MPV percent – along with their respective levels to generate Table 1, shown below. An L-9 matrix is orthogonal, generating test combinations that are independent from one another. This allowed for screening the effect of each parameter with the minimum number of tests—nine.

Table 1: L-9 Generated Test Matrix

Formulation No.	MPV (%)	Solvent Type	Molecular Weight
1	Low	Nonpolar	Low
2	Low	Polar	Medium
3	Low	Nonpolar	High
4	Medium	Polar	Low
5	Medium	Polar	Medium
6	Medium	Nonpolar	High
7	High	Polar	Low
8	High	Nonpolar	Medium
9	High	Polar	High

To test the influence of the three coating preparation parameters on Cl^- diffusion, we employed a DOE matrix to determine the nine experiments needed to examine these variables independently. For input into the matrix, we treated the molecular weight as having three levels: low, medium, and high. The solvent polarity was then treated with two levels—polar and non-polar—and finally, the MPV percent was treated with three levels: low, medium, and high. To formulate the primer, an epoxy resin comprised of di-glycetal ether of bisphenol A was used to form a base. The average molecular weights of the compositions were 177.5 g/mol (low), 181.5 g/mol (medium), or 215 g/mol (high). The viscosity of this base was then lowered by the addition of solvent—either a mixture of ter-butyl acetate and methyl-amyl ketone, which we term polar; or a mixture of benzine and a commercial paint thinner, which we term non-polar. Inhibitors (metals)—typically aluminum, magnesium, and zinc—were then added to the mixture in ratios to give final volume percentages of ~54% (low), ~58% (medium), and ~62% (high) values. This mixture was the first component (A) of the metal-rich primer. To complete the formulation, a second component (B) was prepared just before application, comprising a polyamide and the matching solvent mixture from the first component. Lastly, components A and B were mixed together, agitated, and allowed to sit for a one-hour induction period. For two-part primers, the induction period allowed the mixture to form cross-links. The primer was then applied to the substrate and the entire assembly was cured for 24 hr at 66°C (250°F).

APPARATUS AND PROCEDURE

The testing apparatus was created by affixing 105-degree bend glass tubes to coating-cell glass tubes with epoxy to prevent leakage. The open end of the coating-cell tubes have an o-ring indentation so that a seal can be made to the sample film. Two such assemblies were combined on either side of a sample to form one apparatus. The bent tube served to allow access during the experiment for measurement recording, as shown in Figure 1(c). Samples were coated in silicone to prevent leakage between the sample and o-rings, shown in Figure 1(b). One side of apparatus was filled with deionized (DI) water, while the other side was filled with a 5 wt. % NaCl solution. Each open end of the bend was sealed using a parafilm wrapped cork when measurements were not being performed. We considered the test to start when both sides were

first in contact with solution. For this study, an ISE was used to monitor the chloride ion concentration. Before taking any measurements, both probes were calibrated. The ISE was calibrated every 2 hr (or before each measurement set, whichever occurred first) using 10, 50, 100, 500, and 1000 ppm chloride ion concentration calibration solutions. The 10 wt. % KNO_3 reference solution contained in the ISE probe was replaced once a day prior to the first reading. The pH probe was calibrated daily using 4.01, 7.00, and 10.01 calibration solutions.

Once calibrated, measurements were taken on the DI-side of apparatus after a 60 sec equilibrium time. A total of 3 pH and 5 ppm/mV measurements were taken per reading. Between readings, the probes were rinsed with DI water.

RESULTS

CHLORIDE DIFFUSION

Diffusion data for all the formulations were collected as a function of time: experiments lasted 725-1275 hr. Experiments were terminated when a plateau in measured chloride concentration was observed. To better understand the trends in chloride ion diffusion, the concentration data was fit to a sigmoidal curve which gave chloride concentration as a function of time, given by:

$$C_{Cl}(t) = \frac{M}{1 + e^{-k(t-t_c)}} \tag{1}$$

The constant, M, represents the chloride concentration as time, t, approaches infinity. The time where chloride concentration reaches half its maximum value is characterized by t_c. This point is dependent upon the speed of diffusion of chloride ions, which is represented by the time constant, k. These parameters can be used to calculate t_{90}—the time required for chloride concentration to reach 90 percent of its maximum chloride value. The parameter t_{90} can be used for comparison between two samples that have similar M values. Variable t_{90} was calculated as follows:

$$t_{90} = t_c + \frac{2.2}{k} \tag{2}$$

The fitting was applied to the data collected by the nine independent tests shown in Table 1. Each fit is shown graphically in Figure 2, while each calculated parameter is shown in Table 2.
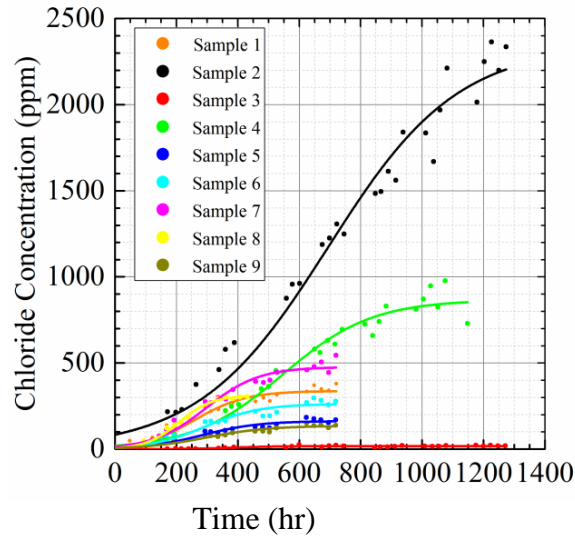
Figure 2: Change in Concentration for Each Sample
(Each Fit Corresponds with Equation 1)

The dependence of chloride concentration on the three different parameters can be examined by the comparison of the different fittings, as shown in Table 2. The first most prominent observation is the stark difference between samples 2 and 3: both ran an excess of 1200 hr—however, sample 3 plateaued near 700 hr while sample 3 has not yet shown strong indication of plateauing. Based on the chloride concentration, it is obvious that sample 2 has allowed many more chloride ions to diffuse through the primer—two orders of magnitude higher than sample 3. Noting the parameters of these two samples, it would seem the MPV percentage has a very small impact on the chloride ion diffusion because the two samples both have low MPV percent. Investigating this trend among the rest of the samples further reinforces this point. Samples 4 and 6 also have a large difference in total chloride ion diffusion despite having the same MPV percent. The same trend can be seen by comparing samples 7 and 9, albeit to a smaller degree. Therefore, it appears MPV percentage does not have a large effect on chloride ion diffusion through metal-rich primers.

Table 2: Variables Calculated from Each Sample, Data Fit to the Sigmoidal Equation
(t_{90} Extrapolated Using Equation 2)

Sample	MPV (%)	Solvent Type	Molecular Weight	M (ppm)	$k * 10^{-3}$ (hr^{-1})	t_c (hr)	t_{90} (hr)
1	Low	Nonpolar	Low	339.7 ± 8.1	12.3 ± 1.0	266.0 ± 11.5	503.6
2	Low	Polar	Medium	2323.5 ± 68.3	5.60 ± 0.4	695.4 ± 24.4	1216.4
3	Low	Nonpolar	High	17.6 ± 0.6	14.1 ± 4.0	379.3 ± 23.8	586.7
4	Medium	Polar	Low	925.0 ± 21.8	6.60 ± 0.4	584.6 ± 15.0	1026.1
5	Medium	Polar	Medium	163.4 ± 5.2	10.1 ± 1.0	286.3 ± 13.7	553.7
6	Medium	Nonpolar	High	266.8 ± 8.2	10.9 ± 1.0	304.5 ± 13.4	572.9
7	High	Polar	Low	462.9 ± 10.2	12.8 ± 1.2	292.9 ± 11.9	521.4
8	High	Nonpolar	Medium	318.2 ± 5.0	19.0 ± 1.3	210.8 ± 5.80	364.7
9	High	Polar	High	135.2 ± 5.0	9.90 ± 0.9	297.7 ± 15.9	591.3

Based on samples 2 and 3, the difference in solvent type may have played a large role in the highly contrasting chloride concentrations. This can be further explored by comparing the average *M* values of the two different solvent types. The nonpolar samples had an average *M* value of 235.592, while the polar samples average value was 802.024. Yet if samples 2 and 3 are removed from the analysis, the averages move much closer to 308.246 for nonpolar and 421.649 for polar. The three samples that allowed the most chloride ion diffusion had a polar solvent type. However, two of three samples that allowed the least amount of chloride ions also had a polar solvent type. Therefore it is likely that solvent polarity may have a synergistic effect with the other variables. As far as other parameters, we observe a slight trend toward lower values in the parameters t_c and t_{90} as a function of *M*—samples with the lowest *M* values had the highest t_c and t_{90} values. This would indicate that high molecular weight conditions act as a barrier for chloride diffusion, since it takes longer for those formulations to reach half and 90%, respectively, of the total chloride concentration allowed.

Comparing the molecular weights of all samples leads to a noticeable trend. Three of the four samples that allowed the least amount of chloride diffusion had a metal-rich primer with a high molecular weight. The fourth sample had a metal-rich primer with a medium molecular weight. Conversely, three of the four samples that allowed the most amount of chloride diffusion had a metal-rich primer with a low molecular weight. These facts indicate that molecular weight has the highest impact on chloride ion diffusion when compared to the other tested parameters. This may be because a metal-rich primer with higher molecular weight consists of larger molecules and thus restricts diffusion channels from forming, inhibiting chloride ions from passing through the primer. Another possible explanation may be that cross-linking is more likely to occur at these high molecular weights. Further studies are needed to confirm these explanations.

pH MEASUREMENTS

Along with concentration, pH data was taken to understand the effects of chloride ion diffusion on pH. The pH data was fit to the following equation:

$$pH(t) = \frac{P_\infty t + P_0 t_i}{t + t_i} \tag{3}$$

where the constant P_∞ signifies the pH when t approaches infinity. The time when pH reaches half of its maximum value is represented by t_i. The value of the pH when time is equal to zero is represented by P_0. The pH data along with the fit according to Equation 3 are shown in Figure 3.
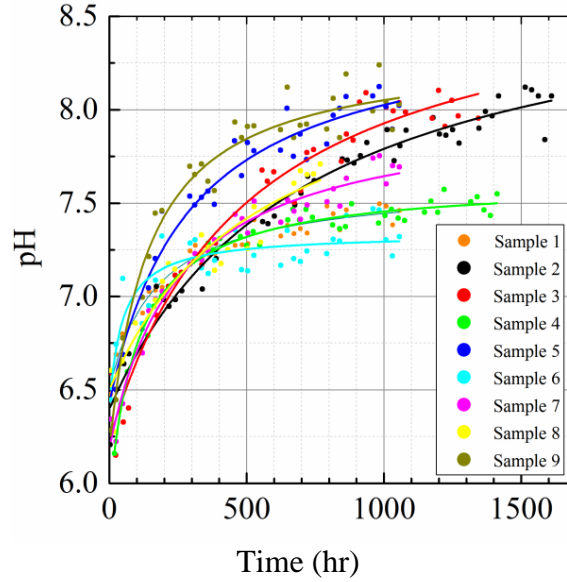

Figure 3: Change in pH Over Time for Each Sample
(Each Fit Corresponds with Equation 3)

The results of the fitting are shown in Table 3. The samples all showed an increase of pH over time, plateauing towards the end of testing. The increase in pH is speculated to be caused by the oxidation of the metal particles in the primer into metal hydroxides. The dissociation of metal hydroxides into the solution then increases the pH over time. The oxidation of metal particles approaches equilibrium and thus the pH begins to level off until it completely plateaus, at which point it has achieved full equilibrium.

Table 3: Variables Calculated from Each Sample pH Fit

Sample	MPV (%)	Solvent Type	Molecular Weight	P_∞	P_0	t_i (hr)
1	Low	Nonpolar	Low	7.62 ± 0.03	6.51 ± 0.04	177.0 ± 27.07
2	Low	Polar	Medium	8.77 ± 0.12	6.40 ± 0.05	701.9 ± 101.8
3	Low	Nonpolar	High	8.77 ± 0.16	6.23 ± 0.08	499.2 ± 99.95
4	Medium	Polar	Low	7.62 ± 0.02	5.92 ± 0.07	107.0 ± 13.46
5	Medium	Polar	Medium	8.49 ± 0.11	6.43 ± 0.08	292.0 ± 59.42
6	Medium	Nonpolar	High	7.34 ± 0.04	6.42 ± 0.14	50.1 ± 24.55
7	High	Polar	Low	8.01 ± 0.07	6.19 ± 0.06	252.5 ± 39.20
8	High	Nonpolar	Medium	8.42 ± 0.42	6.50 ± 0.08	547.1 ± 264.2
9	High	Polar	High	8.32 ± 0.07	6.18 ± 0.09	142.0 ± 24.80

Based on our screening data, it is unclear if pH has any relation to chloride diffusion through metal-rich primers. There is no readily apparent trend that connects pH to chloride ion diffusion. The two highest pH values calculated belonged to the samples that had the highest chloride concentration and smallest chloride concentration. The second lowest pH belongs to the sample with the second highest chloride concentration. These two points reinforce there is no distinct trend between chloride concentration and pH.

There is no observable trend between MPV percentage and pH. Samples 4 and 6 pH values plateau quickly at a low level. They have opposing molecular weights and different solvent types. The only similarity they share is their medium MPV percentage. However, sample 5, which also has a medium MPV percentage, does not plateau quickly and has a very high pH value. This is seen again with samples 2 and 3 having a very high pH value while having a low MPV percentage but sample 1 has the second lowest pH value even though it shares the same MPV percentage.

There is also no trend evident between solvent type and a samples pH value. The average pH of a polar solvent is 8.04 and the average pH of a nonpolar solvent is 8.24. These two values are close and show no strong indication of which solvent may increase or decrease pH. To further reinforce this, the two lowest pH values are very similar but share opposite solvent types. This is also true if we compare the two highest pH values. Samples 2 and 3 share a similar pH but have opposite solvent types. If solvent type had a major impact on pH, these values would be much farther apart.

Molecular weight may play a role in a sample's pH value. Three of the top four pH values come from metal-rich primers that were made with a metal having a medium molecular weight. Three of the bottom four pH values come from a metal-rich primer made with a low molecular weight. This trend is easily identifiable and shows molecular weight has the highest impact on a sample's pH value. Additional data must be collected to determine the source of this trend.

TAGUCHI METHOD

An L-9 orthogonal matrix was applied to the three metal-rich primer variables to generate nine independent test combinations. These combinations provide data on the effect of each parameter without having to physically test each possible arrangement of parameters. Once testing of these independent formations was completed and the fitting parameters were established, the application of the Taguchi method helped determine which metal-rich primer parameter had the greatest effect on the chloride ion diffusion.

The Taguchi method was applied to each of the fitting parameters that were determined by Equation 1, and the results are presented in Table 4. From the Taguchi method, we determined which metal-rich primer variable had the biggest impact on the fitting parameters. Thus we will know which metal-rich primer variable had the biggest impact on the speed of diffusion of chloride ions (k), the maximum amount of chloride ions as time approaches infinity (M), and the time the chloride concentration is at half of its maximum (t_c).

Table 4: Relative Rank of Each Fitting Parameter Using Taguchi Method

Parameter	MPV (%)	Solvent Type	Molecular Weight
M	1.712	0.932	3.150
k	3.435	2.740	5.016
t_{50}	1.641	0.669	3.422
P_∞	8.039	3.663	12.727
Rank	2	3	1

The Taguchi method was consistent between each of the three fitting parameters. Molecular weight has the largest effect on chloride diffusion, while solvent type has the smallest. This partly agrees with the trends noticed in the concentration graph and tables. Trends suggest that molecular weight had the greatest impact on chloride ion diffusion, and this is confirmed by the analysis with the Taguchi method. The Taguchi method results also show MPV percentage has a greater impact than solvent type. However, our analysis of the data trends was not able to distinguish between these two parameters. In the results of the Taguchi method, molecular weight has nearly double the impact of MPV percent and triple the impact of solvent type on chloride ion diffusion. This is shown again by the trends in the previous data. Molecular weight is the only real distinct trend, while MPV percent and solvent type show no strong impact on the data. Supplementary testing is expected to reveal trends in MPV percentage and solvent type data to confirm the analysis done here.

The Taguchi method was also performed on the collected pH data as shown in Table 4. The Taguchi method reports molecular weight has the highest impact on pH, followed by MPV percentage, then solvent type. This somewhat concurs with the trends observed from the data. The trends suggest molecular weight has the largest impact on pH, but none concerning MPV

percentage and solvent type. The Taguchi method results also reveal MPV percentage has a greater impact than solvent type. Additional testing will help identify trends in pH data and help confirm this analysis.

THIS PAGE INTENTIONALLY LEFT BLANK

CONCLUSIONS

While time and material constraints limited the latitude of this experiment, some preliminary trends were identified. The data suggests that for metal-rich organic coating systems. High molecular weight would provide the best protection against chloride diffusion—possibly due to inhibition of diffusion channel formation. Preliminary testing regarding MPV percentage and solvent type was inconclusive, as no trends could be associated to these parameters. However, Taguchi analysis did reveal that, after molecular weight, MPV percentage has the next largest impact and solvent type has the lowest impact on chloride ion diffusion. A trend between pH and chloride ion diffusion could not be ascertained. Further testing is expected to reveal trends in solvent type and MPV percentage variations, which will enable the design of optimal metal-rich organic coatings to allow for the preeminent level of corrosion protection.

THIS PAGE INTENTIONALLY LEFT BLANK

REFERENCES

1. G. Grundmeier, W. Schmidt, M. Stratmann, "Corrosion Protection by Organic Coatings:Electrochemical Mechanism and Novel Methods of Investigation," *Electrochemica Acta* 45, 15-16 (2000): p 2515.

2. J.R. Davis, Corrosion: Understanding the Basics, 1st ed. (Materials Park, OH: ASM International, 2000), pp 363-401.

3. G.W. Walter, "A Critical Review of the Protection of Metals by Paints," Corrosion Science 26, 1 (1986): pp 27-28.

4. N.S. Sangaj, V.C. Malshe, "Permeability of Polymers in Protective Organic Coatings," *Progress in Organic Coatings* 50, 1 (2004): pp 28-29.

5. J. Parks, H. Leidheiser, Jr., "Ionic Migration Through Organic Coatings and its Consequences to Corrosion," *Ind. Eng. Chem. Prod. Res. Dev.* 25, 1 (1986): pp 1-6.

6. F. Deflorian, S. Rossi, "An EIS Study of Ion Diffusion Through Organic Coatings," *Electrochemica Acta* 51, 1 (2006): p 1736.

7. M.L. Zheludkevich, D.G. Shchukin, K.A. Yasakau, H. Möhwald, M.G.S. Ferreira, "Anticorrosion Coatings with Self-Healing Effect Based on Noncontainers Impregnated with Corrosion Inhibitor," *Chem. Mater.* 19,1 (2007): p 402.

8. D.Raps, T. Hack, J. Wehr, M.L. Zheludkevich, A.C. Bastos, M.G.S Ferreira, O. Nuyken, "Electrochemical Study of Inhibitor-Containing Organic-Inorganic Hybrid Coatings on AA2024," *Corrosion Science* 51, 1 (2009): pp 1012-1013.

9. X. Zhang, F.Wang, Y. Du, "Effect of Nano-Sized Titanium Powder Addition on Corrosion Performance of Epoxy Coatings," *Surface & Coatings Technology* 201, 1 (2007): p7241.

10. M. Nematollahi, M. Heidarian, M, Peikari, S.M. Kassiriha, N. Arianpouya, M. Esmaeilpour, "Comparison Between the Effect of Nanoglass Flake Montmorillonite Organoclay on Corrosion Performance of Epoxy Coating," *Corrosion Science* 52, 1 (2010): p 1809.

11. J.R. Scully, "Electrochemical Impedance of Organic-Coated Steel: Correlation of Impedance Parameters with Long-Term Coating Deterioration," J. Electrochem. Soc. 136, 4 (1989): p 9.

THIS PAGE INTENTIONALLY LEFT BLANK

DISTRIBUTION

NAVAIRSYSCOM (AIR-4.3.4.6), Bldg. 2188, Room 206A	(10)
48066 Shaw Road, Patuxent River, MD 20670-1908	
NAVAIRSYSCOM (AIR-5.1V), Bldg. 304, Room 106A	(1)
22541 Millstone Road, Patuxent River, MD 20670-1606	
NAVAIRSYSCOM (AIR-5.1), Bldg. 304, Room 100	(1)
22541 Millstone Road, Patuxent River, MD 20670-1606	
NAVTESTWINGLANT (55TW01A), Bldg. 304, Room 200	(1)
22541 Millstone Road, Patuxent River, MD 20670-1606	
NAVAIRSYSCOM (AIR-4.0T), Bldg. 407, Room 116	(1)
22269 Cedar Point Road, Patuxent River, MD 20670-1120	
DTIC	(1)
8725 John J. Kingman Road, Suite 0944, Ft. Belvoir, VA 22060-6218	